

Proton recoil polarization in exclusive $(e, e'pp)$ reactions

C. Giusti and F. D. Pacati

*Dipartimento di Fisica Nucleare e Teorica dell'Università, Pavia
and Istituto Nazionale di Fisica Nucleare, Sezione di Pavia, Italy*

(November 21, 2018)

The general formalism of nucleon recoil polarization in the $(\vec{e}, e'\vec{N}N)$ reaction is given. Numerical predictions are presented for the components of the outgoing proton polarization and of the polarization transfer coefficient in the specific case of the exclusive $^{16}\text{O}(\vec{e}, e'\vec{pp})^{14}\text{C}$ knockout reaction leading to discrete states in the residual nucleus. Reaction calculations are performed in a direct knockout framework where final-state interactions and one-body and two-body currents are included. The two-nucleon overlap integrals are obtained from a calculation of the two-proton spectral function of ^{16}O where long-range and short-range correlations are consistently included. The comparison of results obtained in different kinematics confirms that resolution of different final states in the $^{16}\text{O}(\vec{e}, e'\vec{pp})^{14}\text{C}$ reaction may act as a filter to disentangle and separately investigate the reaction processes due to short-range correlations and two-body currents and indicates that measurements of the components of the outgoing proton polarization may offer good opportunities to study short-range correlations.

PACS numbers: 24.10.Cn, 25.30.Fj, 27.20.+n

I. INTRODUCTION

It has always been a great challenge of nuclear physics to develop experiments and theoretical models able to explore short-range correlations (SRC). A detailed investigation of these correlations, which are induced by the repulsive components of the nucleon-nucleon (NN) interaction, should give insight into the structure of the interaction of two nucleons in the nuclear medium.

Since a long time electromagnetically induced two-nucleon knockout reactions have been devised as a powerful tool for such investigation, since the probability that a real or virtual photon is absorbed by a pair of nucleons should be a direct measure of the correlations between these nucleons [1,2]. In particular, the $(e, e'pp)$ reaction has been envisaged as the preferential tool for studying SRC in nuclei, since in such a reaction the competing contributions of two-body currents are highly suppressed. Such triple coincidence experiments have been made possible only recently by the progress in accelerator and detector technology. First measurements of the exclusive $^{16}\text{O}(e, e'pp)^{14}\text{C}$ reaction have been performed at NIKHEF in Amsterdam [3–5] and MAMI in Mainz [6]. Investigations on these data [3–7] indicate that resolution of discrete final states provides an interesting tool to disentangle and thus separately investigate contributions of one-body currents, due to SRC, and two-body isobar currents. In particular, direct and clear evidence for SRC has been obtained for the transition to the ground state of ^{14}C . This result opens up good perspectives that further theoretical and experimental efforts on two-nucleon knockout reactions will be able to determine SRC.

Good opportunities to increase the richness of information available from two-nucleon knockout reactions is offered by polarization experiments. In fact, only the use of polarization degrees of freedom allows one to obtain complete information on all possible reaction matrix elements. Reactions with polarized particles depend on a larger number of observables, which are hidden in the unpolarized case, where the sum and/or average over spin states is performed. These observables are represented by new response functions [2], whose determination can impose more severe constraints on theoretical models. In fact, some of these observables are expected to be sensitive to the small components of the transition amplitudes, which without polarization are generally masked by the dominant ones. These small amplitudes often contain interesting information on subtle effects and may thus represent a stringent test of theoretical models. This is the place where polarization observables enter, because in general they contain interference terms of the various matrix elements in different ways. Thus, a small amplitude may be considerably amplified by the interference with a dominant one.

A complete experimental determination of the transition amplitudes requires a long-term program involving the development of new experimental techniques and many different polarization measurements able to separate various sets of structure functions. Unfortunately, some of these measurements are extremely difficult in general and in particular in the case of two-nucleon knockout. Therefore, a complete determination represents at present a too ambitious programme.

In order to exploit, at least partially, the potentiality of polarization measurements, it is possible, however, to select and investigate specific situations corresponding to simpler experiments that appear feasible in the near future. They

should allow one to gain a better control on the reaction mechanism of two-nucleon knockout and hopefully study SRC.

As a first step in the study of spin degrees of freedom in electromagnetic two-nucleon knockout reactions, we consider in this work nucleon recoil polarization. First theoretical predictions have been already presented in Refs. [8,9] within the theoretical model developed by the Gent group. Here we give the most general formalism of $(\vec{e}, e'\vec{N}N)$ reactions in terms of structure functions and polarization observables. Numerical results are shown for the specific case of the exclusive $^{16}\text{O}(\vec{e}, e'\vec{p}p)^{14}\text{C}$ reaction for transitions to the lowest-lying states of the residual nucleus. Calculations have been performed within the theoretical framework of Ref. [7]. This model, that has been successfully applied in the analysis of the first experimental cross sections [4–6], gives a reasonably realistic base to our numerical predictions. Results for the components of the outgoing proton polarization and of the polarization transfer coefficient are presented and discussed in different kinematics. Measurements of the proton recoil polarization require an efficient proton polarimeter and a double scattering. In addition, measurements of the polarization transfer coefficient require also a polarized electron beam. Such experiments are therefore not easy, but seem reasonably within reach of available facilities.

The general formalism is given Sec. II and in Appendix. The numerical results are presented and discussed in Sec. III. Some conclusions are drawn in Sec. IV.

II. NUCLEON RECOIL POLARIZATION IN $(\vec{e}, e'\vec{N}N)$ REACTIONS

In general, the polarization of an outgoing nucleon, which is the expectation value of the spin, can be calculated as [2]

$$\mathbf{P} = \frac{\text{Tr}(MM^\dagger\boldsymbol{\sigma})}{\text{Tr}(MM^\dagger)}, \quad (1)$$

where M is the scattering amplitude of the reaction.

The coincidence cross section of an $(\vec{e}, e'\vec{N}N)$ reaction, where two nucleons, with momenta \mathbf{p}'_1 and \mathbf{p}'_2 and energies E'_1 and E'_2 , are emitted and the polarization of only one nucleon, with spin directed along $\hat{\mathbf{s}}$, is detected can be written

$$\frac{d^5\sigma}{dE'_0 d\Omega'_0 d\Omega'_1 d\Omega'_2 dE'_1} = \sigma_0 \frac{1}{2} \left[1 + \mathbf{P} \cdot \hat{\mathbf{s}} + h(A + \mathbf{P}' \cdot \hat{\mathbf{s}}) \right], \quad (2)$$

where E'_0 is the energy of the outgoing electron, σ_0 the unpolarized differential cross section, \mathbf{P} the outgoing nucleon polarization, h the electron helicity, A the electron analyzing power and \mathbf{P}' the polarization transfer coefficient.

The cross section and the polarization can be expressed in terms of the components of the hadron tensor

$$W_{\alpha\alpha'}^{\mu\nu} = \overline{\sum_i} \sum_f J_\alpha^\mu(\mathbf{q}) J_{\alpha'}^{\nu*}(\mathbf{q}) \delta(E_i - E_f), \quad (3)$$

where α and α' are the eigenvalues of the spin of the considered particle in the given reference frame and \mathbf{q} is the momentum transfer. The quantities $J_\alpha^\mu(\mathbf{q})$ are the Fourier transforms of the transition matrix elements of the nuclear charge-current density operator between initial and final nuclear states

$$J^\mu(\mathbf{q}) = \int \langle \Psi_f | \hat{J}^\mu(\mathbf{r}) | \Psi_i \rangle e^{i\mathbf{q}\cdot\mathbf{r}} d\mathbf{r}. \quad (4)$$

The symmetrical and antisymmetrical combinations of the components of the hadron tensor produce nine spin dependent structure functions. The spin dependence can be explicitated in a spherical basis (see Appendix) as

$$f_{\lambda\lambda'} = h_{\lambda\lambda'}^u + \hat{\mathbf{s}} \cdot \mathbf{h}_{\lambda\lambda'}, \quad (5)$$

where $\hat{\mathbf{s}}$ is the unit vector in the spin space. The structure functions represent the response of the nucleus to the longitudinal and transverse components of the electromagnetic interaction and only depend on the energy and momentum transfer ω and q , the momenta of the two outgoing nucleons p'_1 and p'_2 and the angles γ_1 , between \mathbf{p}'_1 and \mathbf{q} , γ_2 , between \mathbf{p}'_2 and \mathbf{q} , and γ_{12} , between \mathbf{p}'_1 and \mathbf{p}'_2 . When the outgoing nucleon polarization is not detected and the cross section is summed over the spin quantum numbers of the outgoing nucleon, the spin independent structure functions $h_{\lambda\lambda'}^u$ go over to the structure functions $f_{\lambda\lambda'}$ of the unpolarized case [2,12]. Thus, in this case only nine

structure functions are obtained. New structure functions are produced in the polarized case by the components of $\mathbf{h}_{\lambda\lambda'}$

The components of the polarization and of the polarization transfer coefficient are obtained through the structure functions and, involving also the matrix elements of the lepton tensor $\rho_{\lambda\lambda'}$ and $\rho'_{\lambda\lambda'}$ [2], are given by

$$P^i = \frac{\sum_{\lambda\lambda'} \rho_{\lambda\lambda'} h_{\lambda\lambda'}^i}{\sum_{\lambda\lambda'} \rho_{\lambda\lambda'} h_{\lambda\lambda'}^u} \quad (6)$$

and

$$P'^i = \frac{\sum_{\lambda\lambda'} \rho'_{\lambda\lambda'} h_{\lambda\lambda'}^i}{\sum_{\lambda\lambda'} \rho_{\lambda\lambda'} h_{\lambda\lambda'}^u}. \quad (7)$$

The vectors \mathbf{P} and \mathbf{P}' are usually projected onto the basis of unit vectors given by $\hat{\mathbf{L}}$ (parallel to the momentum \mathbf{p}' of the outgoing particle), $\hat{\mathbf{N}}$ (in the direction of $\mathbf{q} \times \mathbf{p}'$) and $\hat{\mathbf{S}} = \hat{\mathbf{N}} \times \hat{\mathbf{L}}$, which define the cm helicity frame of the particle.

The explicit expressions of the cross section in terms of the structure functions and of the structure functions in terms of the components of the hadron tensor can be found in Appendix.

For the $(\vec{e}, e' \vec{N} N)$ reaction in an unrestricted kinematics all the components P^N, P^L, P^S and P'^N, P'^L, P'^S are allowed, as parity conservation does not impose in this case any restrictions. In this general situation 36 structure functions are present: nine spin independent structure functions in σ_0 (h^u) and A (h^u), and nine spin dependent structure functions in each one of the components $i = N, L, S$ of \mathbf{P} (h^i) and \mathbf{P}' (h^i).

This number is reduced in particular situations (see Appendix for more details). When the angle α between the \mathbf{p}'_1 \mathbf{q} plane and the electron scattering plane is equal to zero, all the 36 structure functions are in general non-vanishing, but those of them which are multiplied by $\sin \alpha$ or $\sin 2\alpha$ in Eq. (13) do not contribute to the cross section and to the components of \mathbf{P} and \mathbf{P}' . As a consequence, the condition $\alpha = 0$ reduces to 24 the number of structure functions.

When the vectors $\mathbf{q}, \mathbf{p}'_1, \mathbf{p}'_2$ lie in the same plane, parity conservation combined with the general properties of the hadron tensor reduces the number of non-vanishing structure functions to 18: five in σ_0 and A and 13 in the components of \mathbf{P} and \mathbf{P}' . This result is similar to that obtained for the $(\vec{e}, e' \vec{N})$ reaction in an unrestricted kinematics [2,12].

For a coplanar kinematics, i.e. when the initial and final electrons and the outgoing nucleons lie in the same plane, those of the 18 non-vanishing structure functions which are multiplied by $\sin \alpha$ or $\sin 2\alpha$ do not contribute and the number is reduced to 12, 4 spin independent and 8 spin dependent, and only the components P^N, P'^L and P'^S survive. This result is similar to that obtained for the $(\vec{e}, e' \vec{N})$ reaction in a coplanar kinematics [2,12].

A particular situation occurs in the interesting case of the super-parallel kinematics, where the two outgoing nucleons are ejected parallel and antiparallel to the momentum transfer. In this case only two structure functions, h_{00}^u and h_{11}^u , do not vanish in the unpolarized cross section and three, $h_{01}^N, \bar{h}_{01}^S, h_{11}^L$, when polarization is considered. As a consequence, P^N, P'^L and P'^S are each directly proportional to only one structure function. This result is similar to the one obtained for the $(\vec{e}, e' \vec{N})$ reaction in parallel kinematics [2,12].

It is worthwhile to investigate what happens when final-state interactions (FSI) are neglected and the plane-wave (PW) approximation is used for the outgoing nucleons wave functions.

The behaviour of the hadron tensor under time reversal and parity transformation has the property [10]

$$W^{\mu\nu}(\mathbf{s}, (-)) = W^{\nu\mu}(-\mathbf{s}, (+)), \quad (8)$$

where \mathbf{s} is the spin vector in the ejectile rest frame, and the dependence on the final state boundary condition for incoming $(-)$ and outgoing $(+)$ scattered waves is shown. For nucleon knockout, the $(-)$ condition is appropriate. When the boundary conditions can be ignored, as in the PW approximation, Eq. (8) states that the symmetric part of $W^{\mu\nu}$ is independent of \mathbf{s} and the antisymmetric part is proportional to \mathbf{s} . This is because, owing to the spin- $\frac{1}{2}$ nature of the nucleon, the dependence of $W^{\mu\nu}$ on \mathbf{s} is at most linear. Therefore, in the PW approximation $P^N = P^L = P^S = 0$, while \mathbf{P}' does not vanish.

III. PROTON RECOIL POLARIZATION IN THE $^{16}\text{O}(\vec{e}, e' \vec{p} p)^{14}\text{C}$ REACTION

An experimental separation of the various structure functions would be of great interest, but appears extremely difficult. A measurement of the nucleon recoil polarization would be simpler and less affected by experimental errors, as it is obtained through the determination of asymmetries. Therefore, in this section we present numerical predictions for the outgoing proton polarization \mathbf{P} and the polarization transfer coefficient \mathbf{P}' of the $^{16}\text{O}(\vec{e}, e' \vec{p} p)^{14}\text{C}$

reaction leading to the lowest-lying discrete states in the residual nucleus. This reaction is of particular interest for our investigation, due to the presence of discrete states in the experimental spectrum of the residual nucleus ^{14}C , well separated in energy and that can be separated with high-resolution experiments. Cross sections calculations pointed out that transitions to different states can be differently affected by the two reaction processes due to SRC and two-body currents [7]. Thus, the experimental separation of different final states can act as a filter for the study of the two processes. Recent experiments at NIKHEF and MAMI [3–6] have been able to resolve the lowest-lying states of ^{14}C and have confirmed, in comparison with the theoretical results, the predicted selectivity of the exclusive reaction involving different transitions. In particular, clear evidence of the dominant contribution of SRC has been obtained for the transition to the 0^+ ground state, while the transition to the 1^+ state at 11.31 MeV appears better dominated by the Δ isobar current.

New and complementary information is in principle available from polarization observables. The aim of our investigation is to clarify the sensitivity of \mathbf{P} and \mathbf{P}' to the two competing reaction processes and in particular to SRC.

Calculations have been performed within the same theoretical model [7] used for the analysis of the available cross section data. A detailed description of the theoretical framework can be found in Ref. [7] and in a series of previous papers where the different aspects of the model have been developed [11,13–15]. Here we summarize only the main features.

The transition matrix elements $J^\mu(\mathbf{q})$ in Eq. (4), for an exclusive reaction and under the assumption of a direct knockout mechanism, can be reduced to a form which contains three main ingredients: the two-nucleon overlap integral, the nuclear current and the final-state wave function of the two outgoing nucleons.

In the calculations the scattering state is given by the product of two uncoupled single-particle distorted wave functions, eigenfunctions of a complex phenomenological optical potential which contains a central, a Coulomb and a spin-orbit term.

The nuclear current operator is the sum of a one-body and a two-body part. These two parts correspond to the two reaction processes. In fact, while two nucleons are naturally ejected by a two-body current, even if correlations are not explicitly included in the two-nucleon wave function, they cannot be ejected by a one-body current without correlations. Thus, the contribution of the one-body current is entirely due to correlations. In the calculations the one-body part contains a Coulomb, a convective and a spin term. For pp knockout the two-body current, which is completely transverse, contains only the contributions of non charge-exchange processes with intermediate Δ -isobar configurations in the intermediate state [7,15].

The two-nucleon overlap integrals are taken, for the different final states, from the calculation of the two-proton spectral function of ^{16}O [14], where long-range and short-range correlations are consistently included. They are expressed in terms of a sum of products of relative and cm wave functions. Different components of relative and cm motion contribute to different transitions. They are weighed in the sum by two-proton removal amplitudes calculated within a large shell-model basis. SRC are included in the radial wave functions of relative motion through defect functions, defined by the difference between correlated and uncorrelated relative wave functions, and which are different for different relative states and for different NN potentials.

Therefore, SRC play a different role in different relative states. They are quite strong for the 1S_0 state and much weaker for 3P_j states (the notation $^{2S+1}l_j$, for $l = S, P, \dots$, is here used for the relative states). An opposite effect is given by the two-body Δ current, whose contribution is strongly reduced for 1S_0 pp knockout, since there the generally dominant contribution of that current, due to the magnetic dipole $NN \leftrightarrow N\Delta$ transition, is suppressed [16,17]. Thus, 1S_0 pp knockout is generally dominated by SRC, while the Δ current is more important in 3P_j pp knockout.

This result explains the above mentioned selectivity of the exclusive cross sections involving the transitions to the 0^+ ground state and the 1^+ state. In fact, only 3P relative states, 3P_0 3P_1 3P_2 , contribute for the 1^+ state, whose cross section is generally dominated by the Δ current. The two relative waves 1S_0 and 3P_1 contribute for the 0^+ ground state and it is possible to envisage suitable kinematics where the role of 1S_0 pp knockout and thus of SRC becomes dominant.

In our investigation of polarization observables in the $^{16}\text{O}(\vec{e}, e'\vec{p}p)^{14}\text{C}$ reaction calculations have been performed in different kinematics. In order to obtain a more complete information it is interesting to consider both coplanar and out-of-plane kinematics. Experiments in coplanar kinematics are certainly simpler, but give access only to the components P^N , P'^L and P'^S , while all the components of \mathbf{P} and \mathbf{P}' are present in an out-of-plane kinematics.

A special and interesting case of coplanar kinematics is represented by the so-called super-parallel kinematics [11], where the knocked-out nucleons are detected parallel and anti-parallel to the transferred momentum \mathbf{q} . This kinematics, that has been realized in the experiments at MAMI [6], is favored by the fact that only two structure functions, f_{00} (h_{00}^u) and f_{11} (h_{11}^u), contribute to the unpolarized cross section σ_0 and P^N , P'^L , P'^S are each directly proportional to one structure function: h_{01}^N , h_{11}^L , \bar{h}_{01}^S , respectively.

The unpolarized differential cross section as well as the two unpolarized structure functions in the super-parallel

kinematics of the MAMI experiment have been already shown and discussed in Ref. [7]. The polarization observables P^N , P'^L , P'^S are displayed in Figs. 1 and 2 for the transitions to the 0^+ ground state and the 1^+ state of ^{14}C , respectively, as a function of the recoil (p_B) or missing momentum (p_{2m}), defined by

$$\mathbf{p}_{2m} = \mathbf{p}_B = \mathbf{q} - \mathbf{p}'_1 - \mathbf{p}'_2. \quad (9)$$

In Figs. 1 and 2 the result given by the sum of the one-body and the two-body current is compared with the separate contribution of the one-body current. In Fig. 1, for the transition to the ground state, where effects of SRC are expected to be more relevant, results given by the defect functions for the Bonn-A and Reid NN potentials are compared.

In the calculations each state is characterized by a particular value of the missing energy, given by

$$E_{2m} = \omega - T'_1 - T'_2 - T_B = E_s + E_x, \quad (10)$$

where T'_1 , T'_2 and T_B are the kinetic energies of the two outgoing nucleons and of the residual nucleus, respectively, E_s is the separation energy at threshold for two-nucleon emission and E_x is the excitation energy of the residual nucleus.

In the super-parallel kinematics all possible values of p_B are explored, for a fixed value of the energy and momentum transfer and for a particular final state, changing the values of the kinetic energies of the outgoing nucleons.

An analysis of the results as a function of the recoil momentum appears of particular interest. The shape of the unpolarized differential cross section is determined by the value of the cm orbital angular momentum L of the knocked out pair [1,7,13]. Different components of relative and cm motion contribute to the two-nucleon overlap functions for each final state. The shape of the calculated cross section is therefore driven by the component which gives the major contribution. For the 0^+ state, the 1S_0 and 3P_1 relative waves are combined with $L = 0$ and $L = 1$, respectively; for the 1^+ state the 3P_0 , 3P_1 and 3P_2 relative waves are all combined with $L = 1$ [7]. Cross sections calculations in the considered kinematics indicate that the transition to the 0^+ ground state has an s wave shape, which is due to the major role played by 1S_0 pp knockout, dominated by SRC, for low values of the recoil momentum. The p wave component, which is due to the 3P_1 relative state and is dominated by the Δ current, becomes meaningful only at large values of p_B , beyond 150 – 200 MeV/ c , where the contribution of the s wave becomes much smaller [7]. For the transition to the 1^+ state the cross section has a p wave shape and is almost entirely due to the Δ current [7]. These theoretical findings have been confirmed in comparison with data [6].

The polarization observables displayed in Fig. 1 for the 0^+ state confirm the dominant role of the one-body current up to about 150 – 200 MeV/ c . For larger values of p_B , where the cross section is smaller, the contribution of the Δ current becomes more relevant. This is due to its interference with the one-body current, which is meaningful in the interference longitudinal-transverse structure functions h_{01}^N and \bar{h}_{01}^S in this region of recoil momenta. For the component P'^L , which is proportional to the transverse polarized structure function $h'_{11}{}^L$, the separate contribution of the Δ current is large and of about the same size as that of the one-body current for all the considered values of p_B . Thus, in this case, effects of interference between the one-body current and the two-body current are important over all the momentum distribution.

The results given by the two sets of defect functions from Bonn-A and Reid potentials on the components of P^N , P'^L and P'^S are qualitatively similar. The numerical differences, however, are appreciable and even large at large values of p_B , especially for the component P^N . This effect is predominantly due to the different interference between the one-body current and the Δ current.

The results in Fig. 1 for the transitions to the 0^+ state indicate that in the super-parallel kinematics the considered polarization observables are sizable and sensitive to effects of SRC. The component of the proton recoil polarization P^N appears very well suited to study correlation effects. A measurement of this component would be simpler than a measurement of P'^L and P'^S , which would require also a polarized electron beam. On the other hand, since all the components of \mathbf{P} vanish in the PW approximation, P^N could be also sensitive to the treatment of FSI.

The polarization observables displayed in Fig. 2 for the transition to the 1^+ state are smaller and, as expected, more sensitive to the contribution of the Δ current. The results in Figs. 1 and 2 confirm that different final states in the exclusive $^{16}\text{O}(e, e'pp)^{14}\text{C}$ reaction may act as a filter for the study of the two reaction processes due to SRC and two-body currents.

The super-parallel kinematics represents a special case of coplanar kinematics where only 5 structure functions contribute to the unpolarized and polarized cross sections. In general, in a coplanar kinematics 12 structure functions are present (see Sec. II and Appendix): 4 are contained in the unpolarized cross section σ_0 and 8 in the surviving components of the of the proton recoil polarization P^N and of the polarization transfer coefficient P'^L and P'^S .

As an example, we have here considered a specific kinematical setting included in the first experiment on ^{16}O carried out at NIKHEF [3], with an incident electron energy of 584 MeV, $\omega = 212$ MeV and $q = 300$ MeV/ c . The kinetic energy of the first outgoing proton T'_1 is 137 MeV and the angle $\gamma_1 = 30^\circ$, on the opposite side of the outgoing

electron with respect to the momentum transfer. Changing the angle γ_2 on the other side, different values of the recoil momentum p_B are explored in the range between -250 and 300 MeV/c, including the zero values at $\gamma_2 \simeq 120^\circ$ [7].

The unpolarized cross section has been already discussed in Ref. [7] and is shown again, for the transition to the 0^+ ground state of ^{14}C , in the top panels of Fig. 4. The qualitative features are similar to those obtained in the super-parallel kinematics of the MAMI experiment. For the 0^+ state the shape of the recoil momentum or angular distribution is driven by the component with $L = 0$, that is by 1S_0 pp knockout, and is thus dominated by SRC at low values of p_B . The contribution with $L = 1$, combined with the 3P_1 relative state, which is better driven by the Δ current, is negligible when p_B is low, but becomes meaningful at large values of the recoil momentum, where the contribution of the s wave component is strongly suppressed. In contrast, the transition to the 1^+ state, which contains only 3P relative waves and $L = 1$ cm components, has a p wave shape and is dominated by the Δ current.

The polarization observables P^N , P'^L , and P'^S are displayed, as a function of the angle γ_2 , in Fig. 3 for the transitions to the 0^+ ground state and to the 1^+ state of ^{14}C . For the 0^+ state P^N is large and dominated over all the angular distribution by the one-body current and thus by SRC. The components of the polarization transfer coefficient P'^L and P'^S are also large, but appear better driven by the Δ current. Thus, also in this kinematics the component P^N turns out to be very well suited to study SRC, while in P'^L and P'^S the contribution of the Δ current is relevant and intertwined with that of the one-body current. Therefore, for these two components, whose measurement requires more complicated experiments, the separation of either contribution of the two reaction processes appears difficult.

The comparison between the results with the two kinematical settings in Figs. 1 and 3 for the 0^+ state indicates that in Fig. 3, where a larger number of structure functions contribute, the polarization observables are generally larger and the role of SRC in P^N is dominant over all the distribution. From this point of view, this kinematics seems better suited for the study of SRC with polarization measurements. On the other hand, the role of the Δ current in P'^L and P'^S is more relevant than in the super-parallel kinematics of Fig. 1.

Also in the kinematics of Fig. 3 the polarization observables for the transition to the 1^+ state turn out to be generally smaller than for the 0^+ state. For this transition P^N , P'^L and P'^S are sizable only in the region of low values of p_B , where the cross section has the minimum, and are driven over all the distribution by the Δ current. This result confirms that the transition to the 1^+ state is dominated by two-body currents and indicates that polarization measurements for this final state appear more difficult.

The results of Fig. 3 have been obtained with the defect functions from the Bonn-A potential. Calculations performed with the set of defect functions from the Reid potential give appreciable differences, especially for the 0^+ state and for the observable P^N , which is most affected by correlations. The main qualitative features of the results remain however unchanged with respect to those presented in Fig. 3.

All the components N, L, S of \mathbf{P} and \mathbf{P}' can be explored with an out-of-plane kinematics. Such kinematics can be realized when the angle α , between the \mathbf{p}'_1 \mathbf{q} plane and the electron scattering plane, or the azimuthal angle ϕ of the outgoing proton whose polarization is not considered, or even both α and ϕ are different from zero. In the most general case, where $\alpha \neq 0$ and $\phi \neq 0$, 36 structure functions are obtained (see Sec. II and Appendix). When $\phi \neq 0$, all these structure functions are in general non-vanishing, but if $\alpha = 0$ those of them which are multiplied by $\sin \alpha$ or $\sin 2\alpha$ do not give any contributions. Thus only 24 structure functions are active. If $\phi = 0$, the vectors \mathbf{q} , \mathbf{p}'_1 and \mathbf{p}'_2 lie in the same plane and the structure functions are the same as in coplanar kinematics, but if $\alpha \neq 0$ also those of them which are multiplied by $\sin \alpha$ or $\sin 2\alpha$ contribute. This gives 18 structure functions.

In order to explore all the components of \mathbf{P} and \mathbf{P}' , two examples of out-of-plane kinematics are here considered: $\alpha = 45^\circ$ $\phi = 0^\circ$ and $\alpha = 0^\circ$ $\phi = 30^\circ$. The other kinematical variables are taken as in the coplanar kinematics of Fig. 3. Calculations have been performed only for the transition to the 0^+ ground state, where effects of SRC are known to be most relevant.

The differential cross sections in the two considered out-of-plane kinematics are displayed in Fig. 4 as a function of the angle γ_2 and compared with the cross section of the corresponding coplanar kinematics. The final results are compared in the three cases with the separate contributions of the one-body and the two-body currents and of the 1S_0 and 3P_1 components of relative motion.

In the kinematics with $\alpha = 45^\circ$ the size of the cross section is only slightly lower than in the coplanar kinematics. Also the shapes of the curves given by the separate contributions are similar to those obtained in the coplanar situation. The contribution of the 1S_0 component is, however, reduced and that of 3P_1 enhanced. As a consequence, the role of 3P_1 pp knockout, dominated by the Δ current, is enhanced in the final cross section. This effect slightly changes the shape of the final distribution. On the other hand, when $\alpha = 45^\circ$ the role of the Δ current becomes much more important also on the 1S_0 component, as can be seen from the comparison between the results in the left and right panels. Therefore, in the final cross section the contribution of the Δ current becomes competitive with that of the one-body current even for the transition to the 0^+ state. This is the main difference with respect to the result of the coplanar kinematics and is due to the different role played by the structure functions which are multiplied by factors including the angle α . In particular, a significant role is played by the structure functions multiplied by $\sin \alpha$ and $\sin 2\alpha$, which do not contribute in the coplanar kinematics, and where the effect of the Δ current is important.

In the kinematics with $\phi = 30^\circ$ the cross section is about an order of magnitude lower than in the peak region of the coplanar kinematics and has a different shape. In practice, the peak has disappeared and there is no more evidence of an s shape distribution. In fact, the two contributions of 1S_0 and 3P_1 turn out to be of comparable size in this case. In spite of that, the major role is still played by the one-body current, whose contribution is relevant, even though not dominant, also on the 3P_1 relative wave. A part of the differences with respect to the results of the coplanar kinematics is due to the different structure functions and to their dependence on the angle ϕ . The main reason of the differences, however, can be attributed to a kinematic effect. In fact, when the outgoing nucleon is taken out of the plane, different values of the recoil momentum p_B are obtained in the considered range of γ_2 . In particular, low values in the range between -160 and 160 MeV/ c are forbidden. Thus, the main source of difference with respect to the coplanar situation is that the region of momenta between -160 and 160 MeV/ c , where the s wave has the maximum and the p wave a minimum, has been cut. This explains the different shape of the angular distributions in the top and bottom panels of Fig. 4.

The components of \mathbf{P} and \mathbf{P}' in the two kinematics with $\alpha = 45^\circ$ and $\phi = 30^\circ$ are displayed in Figs. 5 and 6, respectively.

In Fig. 5, with $\alpha = 45^\circ$, the components P^N , P'^L and P'^S , already present in coplanar kinematics, are significantly different from those displayed in Fig. 3 for the same transition. The differences are larger for P^N and P'^L . The Δ current gives the major contribution to P'^L and P'^S . The one-body current gives the main contribution to P^N , but in this kinematics the effect of the Δ current is meaningful also on this polarization component and larger than in coplanar kinematics. Of the three observables P'^N , P^L and P^S , which are present only in an out-of-plane kinematics, P'^N is small, while P^L and P^S are sizable. However, both contributions of SRC and two-body currents are large and intertwined in these polarization components. Therefore, the kinematics with $\alpha = 45^\circ$ does not seem particularly well suited to disentangle the two reaction processes and study SRC.

Correlation effects are much more important in Fig. 6, for the kinematics with $\phi = 30^\circ$. In this case all the components of the outgoing proton polarization \mathbf{P} are sizable and driven by the one-body current, which gives the main contribution also to P'^N . This component of the polarization transfer coefficient, however, is small also in this kinematics. The other components P'^L and P'^S are large, but also in this case strongly affected by both contributions of the two reaction processes due to SRC and two-body currents.

IV. SUMMARY AND CONCLUSIONS

In this paper we have discussed the general properties of the nucleon recoil polarization in the $(\vec{e}, e'\vec{N})N$ reaction. In the most general situation no restrictions are due to parity conservation and 36 structure functions are active, more than in the $(\vec{e}, e'\vec{N})$ reaction, where parity conservation reduces the number of structure functions available in an unconstrained kinematics to 18. The same formal situation is obtained in $(\vec{e}, e'\vec{N})N$ only when the momenta of the two outgoing nucleons and the momentum transfer lie in the same plane. A minor number of structure functions can be obtained in more restricted kinematics: 12 in a coplanar kinematics, as in the coplanar kinematics of $(\vec{e}, e'\vec{N})$, and 5 in the special case of the super-parallel kinematics, as in the parallel kinematics of $(\vec{e}, e'\vec{N})$.

An experimental determination of the structure functions would be of great interest, but appears at present extremely difficult. In order to exploit the potentiality of polarization measurements to increase the richness of information available in two-nucleon knockout reactions, it is anyhow possible to envisage other interesting polarization experiments which appear more feasible. As an example, a measurement of the nucleon recoil polarization, which is obtained through the determination of asymmetries, should be reasonably within reach of available facilities.

A complete investigation of all the components of the outgoing nucleon polarization \mathbf{P} and of the polarization transfer coefficient \mathbf{P}' , which implies also a polarized electron beam, requires out-of-plane experiments. In the simpler case of a coplanar kinematics only the components P^N , P'^L and P'^S are available, as in the coplanar kinematics of the $(\vec{e}, e'\vec{N})$ reaction. Moreover, as in $(\vec{e}, e'\vec{N})$, all the components of the outgoing nucleon polarization \mathbf{P} vanish in the PW approximation.

The aim of this work was to explore the capability of polarization measurements to disentangle and separately investigate the two reaction processes due to correlations and two-body currents. With this aim and within our theoretical framework, we have checked the sensitivity of \mathbf{P} and \mathbf{P}' to the two competing processes.

Numerical predictions have been presented for the specific case of the exclusive $^{16}\text{O}(\vec{e}, e'\vec{p}p)^{14}\text{C}$ reaction leading to the lowest-lying discrete states of the residual nucleus. Our results confirm that the contribution of SRC as compared with that of the Δ current depends on the final state of the residual nucleus and that the transition to the ground state of ^{14}C is particularly sensitive to correlation effects. Calculations performed in the coplanar kinematical settings realized for the cross section measurements at NIKHEF and MAMI indicate that for the transition to the ground state the major contribution to the only surviving component of the outgoing proton polarization, perpendicular to

the plane, is given by correlations, while effects of two-body currents are almost negligible. In contrast, these effects are much more important or even dominant on the components of the polarization transfer coefficient.

In more complicated non coplanar kinematics the number of available observables increases, but their sensitivity to nuclear correlations is reduced. It is possible to envisage particular conditions where correlation effects are dominant, but they correspond to situations where measurements are more difficult and cross sections generally smaller.

In conclusion, we believe that a combined measurement of cross sections and polarizations in $(\vec{e}, e'\vec{p}p)$ reactions would provide a unique tool to determine short-range nuclear correlations and could positively contribute to clarify the behaviour of the short-range interaction of nucleons in the nuclear medium.

The analysis of polarization observables can be extended to other electromagnetic two-nucleon knockout reactions, such as $(e, e'pn)$, (γ, pn) and (γ, pp) .

Recent calculations [19] have shown that the cross section of the exclusive $^{16}\text{O}(\vec{e}, e'\vec{p}n)^{14}\text{N}$ reaction are sensitive to details of the nuclear correlations considered and in particular to the presence of the tensor component. Therefore, a study of polarization observables in the $(e, e'pn)$ reaction would be of particular interest for the study of tensor correlations.

Cross sections and photon asymmetries calculated for both (γ, pp) and (γ, pn) knockout reactions are dominated by two-body currents and only slightly affected by correlation effects [16]. Thus, reactions induced by real photons do not seem particularly well suited to study correlations, but are anyhow interesting to give complementary information on other theoretical ingredients, for instance on the nuclear currents. Moreover, polarization observables could amplify the role of small amplitudes and of subtle effects hidden in the unpolarized case. Therefore, also (γ, pp) and (γ, pn) reactions deserve a careful investigation.

APPENDIX

The components of the hadron tensor $W^{\mu\nu}$ are to be restricted by the conditions of current conservation

$$W^{\mu\nu}q_\mu = W^{\mu\nu}q_\nu = 0. \quad (11)$$

Therefore, the sixteen components of the tensor are reduced to nine independent quantities. By separating the symmetrical and antisymmetrical terms, one obtains six symmetrical and three antisymmetrical independent components.

A spherical basis can be used and defined by the four-vectors

$$\epsilon_{\pm 1}^\mu = \mp \frac{1}{\sqrt{2}}(0, 1, \pm i, 0), \quad \epsilon_0^\mu = \left(\frac{|\mathbf{q}|}{Q}, 0, 0, \frac{\omega}{Q}\right), \quad (12)$$

where $Q^2 = |\mathbf{q}|^2 - \omega^2$. (Note that this spherical basis is consistent with Ref. [2], and is different from the one used in other papers, where $\epsilon_0^\mu = (1, 0, 0, 0)$.)

Then, nine structure functions are obtained as a function of the hadron tensor components [2,11]. Their expressions are given in Table 1, in the reference frame where the z axis is taken parallel to \mathbf{q} and the momentum \mathbf{p}'_1 lies in the \mathbf{xz} plane.

The triple coincidence cross section for the electron induced reaction where two nucleons are emitted is obtained from the contraction between the lepton tensor and the hadron tensor as a linear combination of the nine structure functions [2,11]

$$\begin{aligned} \frac{d^5\sigma}{dE'_0 d\Omega'_0 d\Omega'_1 d\Omega'_2 dE'_1} &= \sigma_M \Omega_f f_{\text{rec}} \sum_{\lambda\lambda'} \{ \rho_{\lambda\lambda'} f_{\lambda\lambda'} + h \rho'_{\lambda\lambda'} f'_{\lambda\lambda'} \} \\ &= K \Omega_f f_{\text{rec}} \left\{ \epsilon_L f_{00} + f_{11} + \sqrt{\epsilon_L(1+\epsilon)} (f_{01} \cos \alpha + \bar{f}_{01} \sin \alpha) \right. \\ &\quad \left. - \epsilon (f_{1-1} \cos 2\alpha + \bar{f}_{1-1} \sin 2\alpha) \right. \\ &\quad \left. + h \left[\sqrt{\epsilon_L(1-\epsilon)} (f'_{01} \sin \alpha + \bar{f}'_{01} \cos \alpha) + \sqrt{1-\epsilon^2} f'_{11} \right] \right\}, \quad (13) \end{aligned}$$

where σ_M is the Mott scattering cross section,

$$\Omega_f = |\mathbf{p}'_1| E'_1 |\mathbf{p}'_2| E'_2, \quad (14)$$

$$f_{\text{rec}}^{-1} = 1 - \frac{E'_2}{E_r} \frac{\mathbf{p}'_2 \cdot \mathbf{p}_r}{|\mathbf{p}'_2|^2}, \quad (15)$$

where E_r and \mathbf{p}_r are the relativistic energy and momentum of the residual nucleus,

$$K = \frac{e^4}{16\pi^2} \frac{E'_0}{Q^2 E_0 (1 - \epsilon)}, \quad (16)$$

$$\epsilon = \left(1 + 2 \frac{|\mathbf{q}|^2}{Q^2} \tan^2 \frac{\theta}{2}\right)^{-1}, \quad (17)$$

$$\epsilon_L = \frac{Q^2}{|\mathbf{q}|^2} \epsilon \quad (18)$$

and E_0 and E'_0 are the energies of the incident and outgoing electrons. The components of the lepton tensor $\rho_{\lambda\lambda'}$ and $\rho'_{\lambda\lambda'}$ can be deduced from Eq. (13).

The structure functions depend on the kinematical variables of the particular process under investigation. Even if a large number of variables are involved, at most four independent four-momenta are available in the Lorentz frame. Therefore, the hadron tensor can be expanded on the basis of four independent variables [2]. In the case of two-nucleon emission different choices are possible. One can refer to the target four-momentum P^μ , the momentum transfer q^μ , the ejectile four-momentum $p_1'^\mu$ and the four vector

$$\xi^\mu = \epsilon^{\alpha\beta\gamma\mu} q_\alpha p_{1\beta}' P_\gamma. \quad (19)$$

The expansion coefficients can depend on the invariants $Q^2, P \cdot q, q \cdot p_1', q \cdot p_2', P \cdot p_1', P \cdot p_2', p_1' \cdot p_2'$ and $\xi \cdot s_1$, where s_1 is the spin of the outgoing nucleon with momentum \mathbf{p}'_1 , which are scalars and $P \cdot s_1, q \cdot s_1, p_2' \cdot s_1$ and $\xi \cdot p_2'$, which are pseudoscalars. It is worthwhile to notice that both scalars and pseudoscalars, both dependent on and independent of s_1 , are available.

The four-vector s_1 , in the reference frame where $\mathbf{p}'_1 = 0$, is given by $s_1 = (0, \mathbf{s}_1)$ and can be boosted in the laboratory frame as [10]

$$s_1^\mu = \left(\frac{\mathbf{s}_1 \cdot \mathbf{p}'_1}{m}, \mathbf{s}_1 + \frac{\mathbf{s}_1 \cdot \mathbf{p}'_1}{m(E'_1 + m)} \mathbf{p}'_1 \right). \quad (20)$$

Therefore, we obtain the invariants

$$\xi \cdot s_1 = M_T \mathbf{q} \times \mathbf{p}'_1 \cdot \mathbf{s}_1, \quad (21)$$

$$P \cdot s_1 = \frac{M_T}{m} \mathbf{p}'_1 \cdot \mathbf{s}_1, \quad (22)$$

where m is the nucleon mass and M_T the target mass, and

$$q \cdot s_1 = \left(\frac{\omega}{m} - \frac{\mathbf{q} \cdot \mathbf{p}'_1}{m(E'_1 + m)} \right) \mathbf{p}'_1 \cdot \mathbf{s}_1 - \mathbf{q} \cdot \mathbf{s}_1. \quad (23)$$

It is clear from the above equations that $\xi \cdot s_1$ is proportional to $\hat{\mathbf{N}} \cdot \mathbf{s}_1$, $P \cdot s_1$ to $\hat{\mathbf{L}} \cdot \mathbf{s}_1$ and $q \cdot s_1$ has a component proportional to $\hat{\mathbf{S}} \cdot \mathbf{s}_1$. Since we can obtain from these invariants both scalars and pseudoscalars which linearly contain the spin, it follows that no restrictions due to parity conservation can in general be derived concerning the dependence of the different structure functions on the components of the spin, in contrast with what happens in the $(\vec{e}, e' \vec{N})$ reaction.

These restrictions are recovered in the particular case of a reaction where the outgoing nucleon momenta \mathbf{p}'_1 and \mathbf{p}'_2 and the momentum transfer \mathbf{q} lie all in the same plane. In this case the invariant $\xi \cdot p_2' = 0$, and neither scalars proportional to $\hat{\mathbf{L}} \cdot \mathbf{s}_1$ and $\hat{\mathbf{S}} \cdot \mathbf{s}_1$, nor pseudoscalars proportional to $\hat{\mathbf{N}} \cdot \mathbf{s}_1$ are obtained. This result is independent of the electron plane and corresponds to the typical situation, in an unrestricted kinematics, of the $(\vec{e}, e' \vec{N})$ reaction.

In general, for the $(\vec{e}, e' \vec{N}N)$ reaction, the dependence of the structure functions on the spin can be explicated remembering that for a particle with spin $\frac{1}{2}$ only a linear dependence is allowed, as

$$f_{\lambda\lambda'} = h_{\lambda\lambda'}^u + \hat{\mathbf{s}} \cdot \mathbf{h}_{\lambda\lambda'}, \quad (24)$$

where \hat{s} is the unit vector in the spin space. Thus, when the polarization of the outgoing nucleon is considered, 36 structure functions $h_{\lambda\lambda'}^u$ and $h_{\lambda\lambda'}^i$ are obtained. The explicit expressions of these structure functions in terms of the components of the hadron tensor $W_{\alpha\alpha'}^{\mu\nu}$ can be easily obtained from Table I, by simply substituting the quantities $W^{\mu\nu}$, wherever they appear, with the following expressions:

$$\begin{aligned}
W_{++}^{\mu\nu} + W_{--}^{\mu\nu} & \text{ for } i = u, \\
W_{+-}^{\mu\nu} + W_{-+}^{\mu\nu} & \text{ for } i = x, \\
i(W_{++}^{\mu\nu} - W_{--}^{\mu\nu}) & \text{ for } i = y, \\
W_{++}^{\mu\nu} - W_{--}^{\mu\nu} & \text{ for } i = z.
\end{aligned} \tag{25}$$

Usually, the quantities $h_{\lambda\lambda'}$ and $h'_{\lambda\lambda'}$ are projected onto the basis of unit vectors \hat{N} , \hat{L} and \hat{S} defined in Sec. II and the structure functions are thus given for the components $i = N, L, S$.

In the most general situation all the 36 structure functions do not vanish. When the electrons are on the \mathbf{xz} plane, i.e. when $\alpha = 0$, the structure functions which are multiplied by $\sin\alpha$ or $\sin 2\alpha$ in Eq. (13) do not contribute. In this case only 24 structure functions contribute to the cross section and polarizations. When the two outgoing nucleons and the momentum transfer lie in the same plane, we recover formally the typical situation of the $(\vec{e}, e'\vec{N})$ reaction [2,12] and only 18 structure functions do not vanish. In all these cases all the components of the polarization and of the polarization transfer coefficient are in principle different from zero. In a coplanar kinematics, i.e. when the momenta of the electrons and of the outgoing nucleons lie in the same plane, we recover the typical situation of the $(\vec{e}, e'\vec{N})$ reaction in coplanar kinematics, where only 12 structure functions contribute and only P^N, P^L and P^S do not vanish. Finally, in the super-parallel kinematics only 5 structure functions survive, as in the parallel kinematics of the $(\vec{e}, e'\vec{N})$ reaction.

- [1] K. Gottfried, Nucl. Phys. **5**, 557 (1958); Ann. of Phys. **21**, 63 (1963).
- [2] S. Boffi, C. Giusti, F. D. Pacati and M. Radici, *Electromagnetic Response of Atomic Nuclei*, Oxford Studies in Nuclear Physics (Clarendon Press, Oxford, 1996).
- [3] C. J. G. Onderwater, K. Allaart, E. C. Aschenauer, Th. S. Bauer, D. J. Boersma, E. Cisbani, S. Frullani, F. Garibaldi, W. J. W. Geurts, D. Groep, W. H. A. Hesselink, M. Iodice, E. Jans, N. Kalantar-Nayestanaki, W. -J. Kasdorp, C. Kormanyos, L. Lapikás, J. J. van Leeuwe, R. De Leo, A. Misiejuk, A. R. Pellegrino, R. Perrino, R. Starink, M. Steenbakkens, G. van der Steenhoven, J. J. M. Steijger, M. A. van Uden, G. M. Urciuoli, L. B. Weinstein, and H. W. Willering, Phys. Rev. Lett. **78**, 4893 (1997).
- [4] C. J. G. Onderwater, K. Allaart, E. C. Aschenauer, Th. S. Bauer, D. J. Boersma, E. Cisbani, W. H. Dickhoff, S. Frullani, F. Garibaldi, W. J. W. Geurts, C. Giusti, D. Groep, W. H. A. Hesselink, M. Iodice, E. Jans, N. Kalantar-Nayestanaki, W. -J. Kasdorp, C. Kormanyos, L. Lapikás, J. J. van Leeuwe, R. De Leo, A. Misiejuk, H. Müther, F. D. Pacati, A. R. Pellegrino, R. Perrino, R. Starink, M. Steenbakkens, G. van der Steenhoven, J. J. M. Steijger, M. A. van Uden, G. M. Urciuoli, L. B. Weinstein, and H. W. Willering, Phys. Rev. Lett. **81**, 2213 (1998).
- [5] R. Starink, M. F. Van Batenburg, E. Cisbani, W. H. Dickhoff, S. Frullani, F. Garibaldi, C. Giusti, D. L. Groep, P. Heimberg, W. H. A. Hesselink, M. Iodice, E. Jans, L. Lapikás, R. De Leo, C. J. G. Onderwater, F. D. Pacati, R. Perrino, J. Ryckebusch, M. F. M. Steenbakkens, J. A. Templon, G. -M. Urciuoli and L. B. Weinstein, Phys. Lett. **B**, (2000) in press.
- [6] G. Rosner, *Conference on Perspectives in Hadronic Physics*, eds. S. Boffi, C. Ciofi degli Atti, and M. M. Giannini (World Scientific, Singapore, 1998) p.185; Proceedings of the 10th Mini-Conference on Studies of Few-Body Systems with High Duty-Factor Electron Beams, NIKHEF, Amsterdam 1999, p.95.
- [7] C. Giusti, F. D. Pacati, K. Allaart, W. J. W. Geurts, W. H. Dickhoff and H. Müther, Phys. Rev. C **57**, 1691 (1998).
- [8] J. Ryckebusch, W. Van Nespén and D. Debruyne, Phys. Lett. B **441**, 1 (1998).
- [9] J. Ryckebusch, D. Debruyne and W. Van Nespén, Phys. Rev. C **57**, 1319 (1998).
- [10] A. Picklesimer and J. W. Van Orden, Phys. Rev. C **35**, 266 (1987).
- [11] C. Giusti and F. D. Pacati, Nucl. Phys. **A535**, 573 (1991); Nucl. Phys. **A571**, 694 (1994).
- [12] C. Giusti and F. D. Pacati, Nucl. Phys. **A504**, 373 (1989).
- [13] C. Giusti and F. D. Pacati, Nucl. Phys. **A615**, 373 (1997).
- [14] W. J. W. Geurts, K. Allaart, W. H. Dickhoff and H. Müther, Phys. Rev. C **54**, 1144 (1996).
- [15] P. Wilhelm, H. Arenhövel, C. Giusti, and F. D. Pacati, Z. Phys. A **359**, 467 (1997).
- [16] C. Giusti and F. D. Pacati, Nucl. Phys. **A641**, 297 (1998).

- [17] P. Wilhelm, J. A. Niskanen and H. Arenhövel, Nucl. Phys. **A597**, 613 (1996).
 [18] A. Nadasen, P. Schwandt, P. P. Singh, W. W. Jacobs, A. D. Bacher, P. T. Debevec, M. .D. Kaichuk and J. T. Meek, Phys. Rev. C **23**, 1023 (1981).
 [19] C. Giusti, H. Müther, F. D. Pacati and M. Stauf, Phys. Rev. C **60**, 054608 (1999).

| | |
|---|---|
| $f_{00} = \frac{ \mathbf{q} ^2}{Q^2} W^{00}$ | $f_{11} = W^{xx} + W^{yy}$ |
| $f_{01} = -\frac{ \mathbf{q} }{Q} \sqrt{2} (W^{0x} + W^{x0})$ | $\bar{f}_{01} = \frac{ \mathbf{q} }{Q} \sqrt{2} (W^{0x} + W^{x0})$ |
| $f_{1-1} = W^{yy} - W^{xx}$ | $\bar{f}_{1-1} = W^{xy} + W^{yx}$ |
| $f'_{01} = \frac{ \mathbf{q} }{Q} i \sqrt{2} (W^{0x} - W^{x0})$ | $\bar{f}'_{01} = \frac{ \mathbf{q} }{Q} i \sqrt{2} (W^{0y} - W^{y0})$ |
| $f'^{11} = -i(W^{xy} - W^{yx})$ | |

TABLE I. Structure functions in terms of the components of the hadron tensor.

FIG. 1. The components of the outgoing proton polarization P^N and of the polarization transfer coefficient P'^L and P'^S of the $^{16}\text{O}(\bar{e}, e'\bar{p}p)^{14}\text{C}$ reaction as a function of the recoil momentum p_B for the transition 0^+ ground state of ^{14}C ($E_{2m} = 22.33$ Mev) in the super-parallel kinematics ($\gamma_1 = 0^\circ$, $\gamma_2 = 180^\circ$) with an incident electron energy $E_0 = 855$ MeV, $\omega = 215$ MeV and $q = 316$ MeV/c. Different values of p_B are obtained changing the kinetic energies of the outgoing protons. Positive (negative) values of p_B refer to situations where \mathbf{p}_B is parallel (antiparallel) to \mathbf{q} . Polarization is considered for the proton characterized by the momentum \mathbf{p}'_1 . The dashed lines give the contribution of the one-body current, the solid line the sum of the one-body and the two-body Δ -current. The defect functions for the Bonn-A and Reid NN potentials are used in the left and right panels, respectively. The optical potential is taken from Ref. [18].

FIG. 2. The components of the outgoing proton polarization P^N and of the polarization transfer coefficient P'^L and P'^S of the $^{16}\text{O}(\bar{e}, e'\bar{p}p)^{14}\text{C}$ reaction as a function of the recoil momentum p_B for the transition 1^+ state of ^{14}C at 11.31 MeV ($E_{2m} = 33.64$ Mev) in the same kinematics and conditions and with same line convention as in Fig. 1. The defect functions for the Bonn-A NN potential are used.

FIG. 3. The components of the outgoing proton polarization P^N and of the polarization transfer coefficient P'^L and P'^S of the $^{16}\text{O}(\bar{e}, e'\bar{p}p)^{14}\text{C}$ reaction as a function of the angle γ_2 for the transitions to the 0^+ ground state (left panels) and the 1^+ state at 11.31 MeV (right panels) of ^{14}C . The incident electron energy is $E_0 = 584$ MeV, $\omega = 212$ MeV and $q = 300$ MeV/c, $T'_1 = 137$ MeV and $\gamma_1 = 30^\circ$, on the opposite side of the outgoing electron with respect to the momentum transfer. Polarization is considered for the proton characterized by the kinetic energy T'_1 and angle γ_1 . The defect functions for the Bonn-A potential and the optical potential of Ref. [18] are used.

FIG. 4. The differential cross section of the $^{16}\text{O}(e, e'pp)^{14}\text{C}$ reaction as a function of the angle γ_2 for the transition to the 0^+ ground state of ^{14}C in the same coplanar kinematics as in Fig. 3 (top panels) and in two different out-of-plane kinematics with $\alpha = 45^\circ$ and with the azimuthal angle of the second outgoing proton $\phi = 30^\circ$. Defect functions and optical potential as in Fig. 3. The separate contributions of the one-body and the two-body Δ currents are shown by the dashed and dotted lines, respectively in the left panels. Separate contributions of the different partial waves of relative motion 1S_0 and 3P_1 are shown by the dashed and dotted lines, respectively, in the right panels. The solid lines are the same in the left and right panels and give the final result sum of the various contributions.

FIG. 5. The components of the outgoing proton polarization \mathbf{P} (left panels) and of the polarization transfer coefficient \mathbf{P}' (right panels) for the same reaction and in the same out-of-plane kinematics with $\alpha = 45^\circ$ and with the same conditions as in Fig. 4. Line convention as in Fig. 1. Polarization is considered for the proton characterized by the momentum \mathbf{p}'_1 .

FIG. 6. The components of the outgoing proton polarization \mathbf{P} (left panels) and of the polarization transfer coefficient \mathbf{P}' (right panels) for the same reaction and in the same out-of-plane kinematics with $\phi = 30^\circ$ and with the same conditions as in Fig. 4. Line convention as in Fig. 1. Polarization is considered for the proton characterized by the momentum \mathbf{p}'_1 .

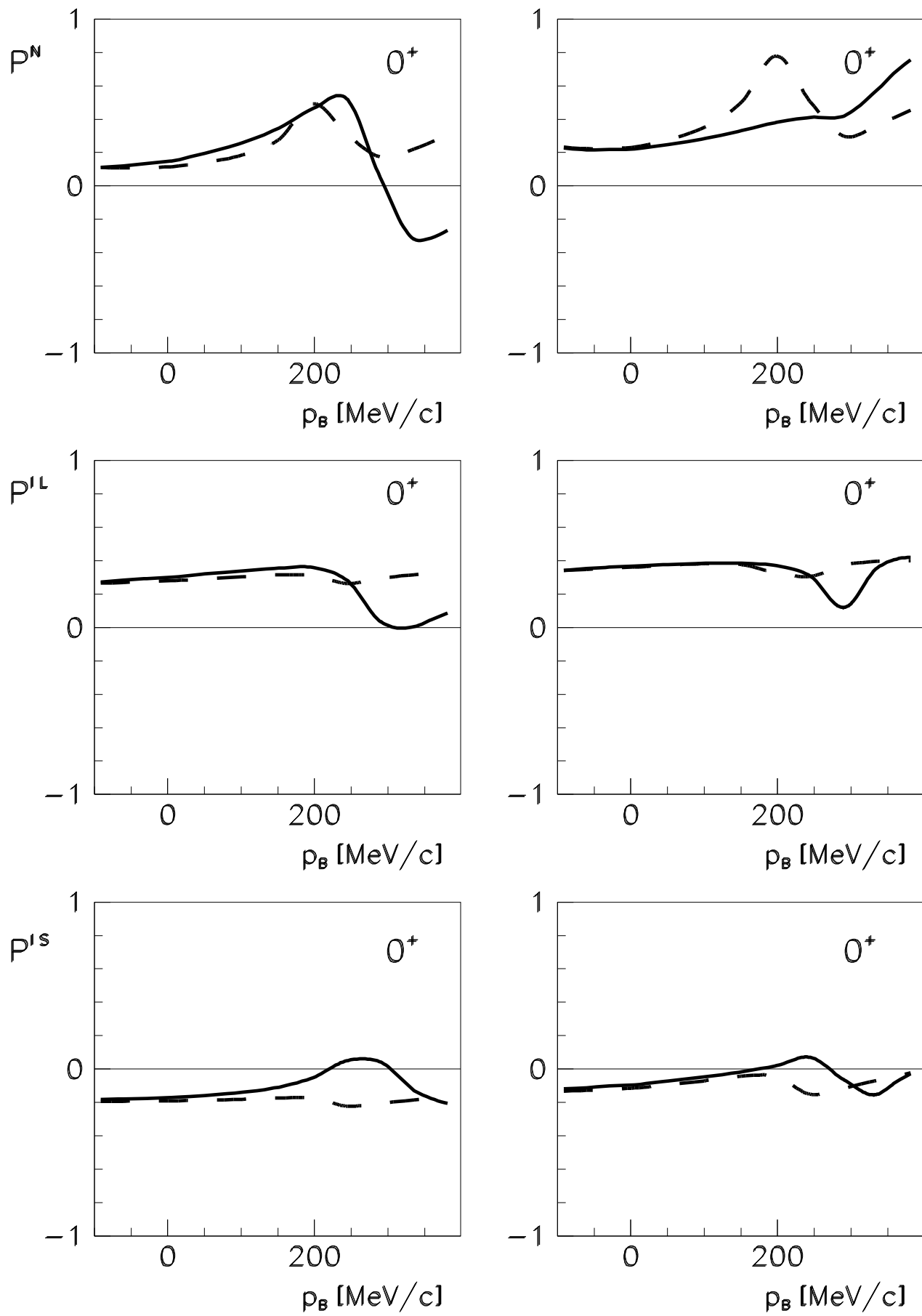


Fig. 1

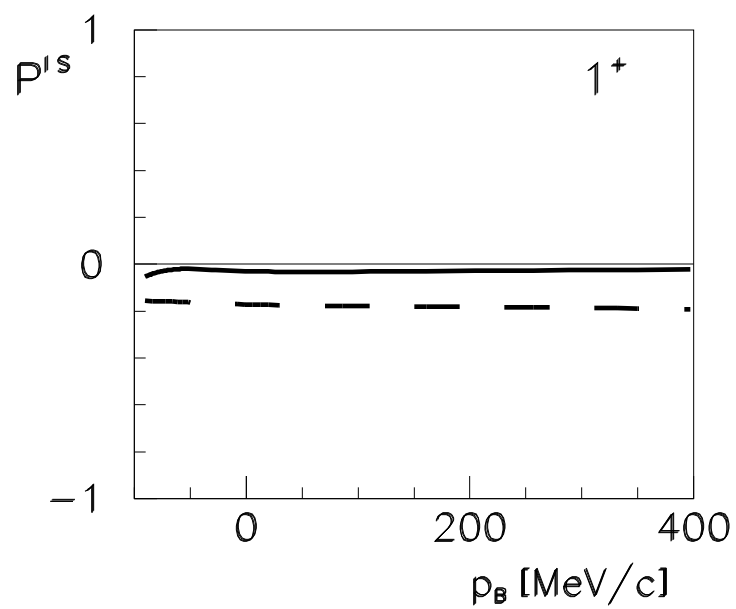
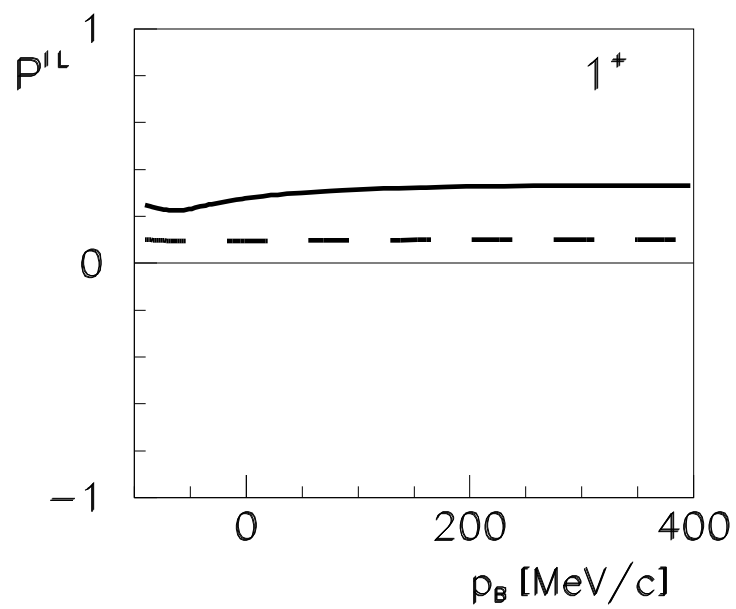
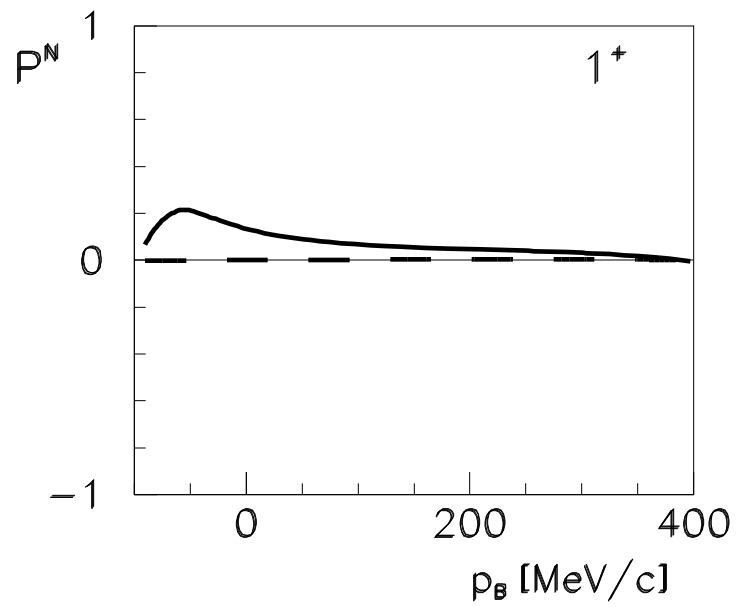


Fig. 2

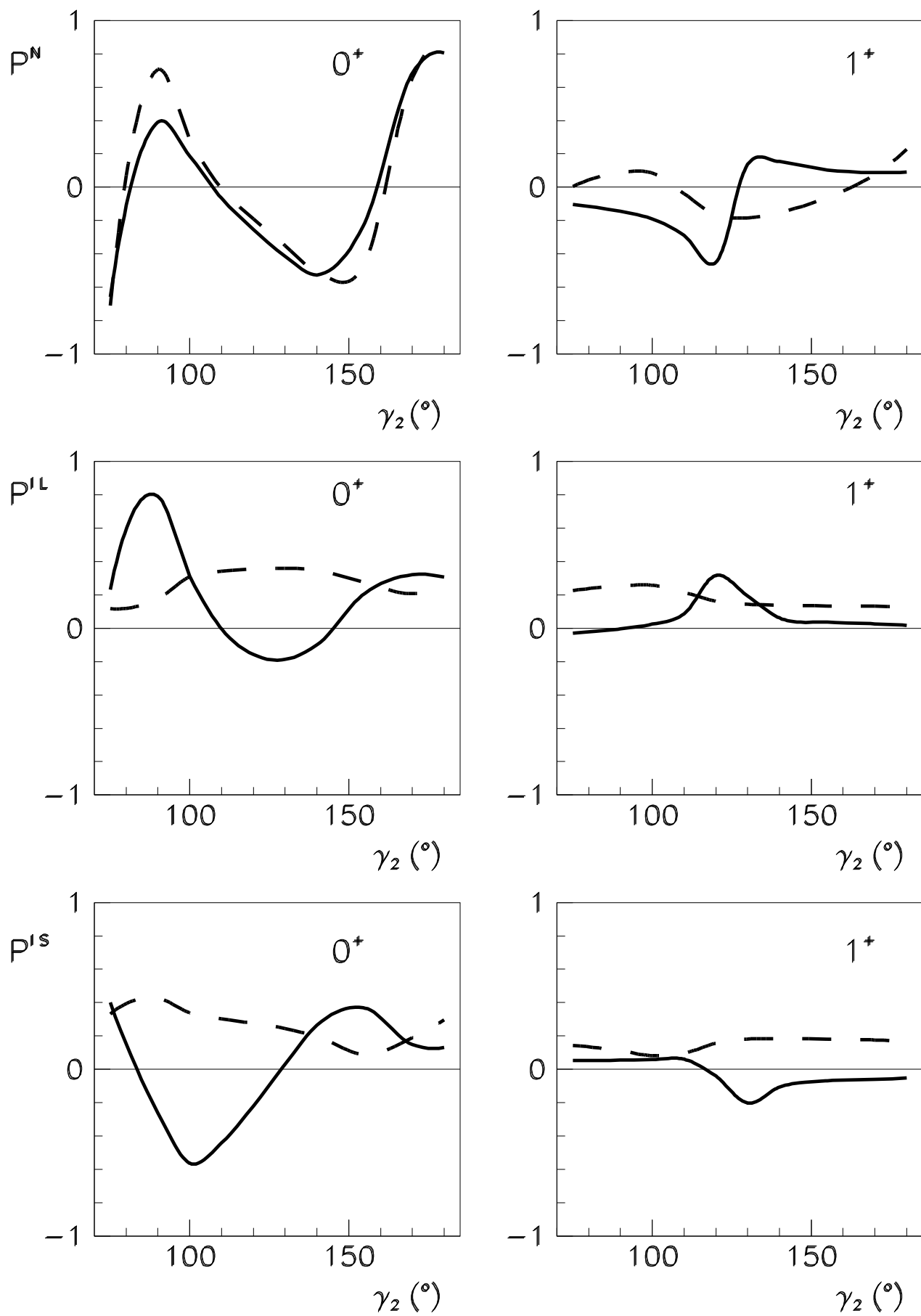


Fig. 3

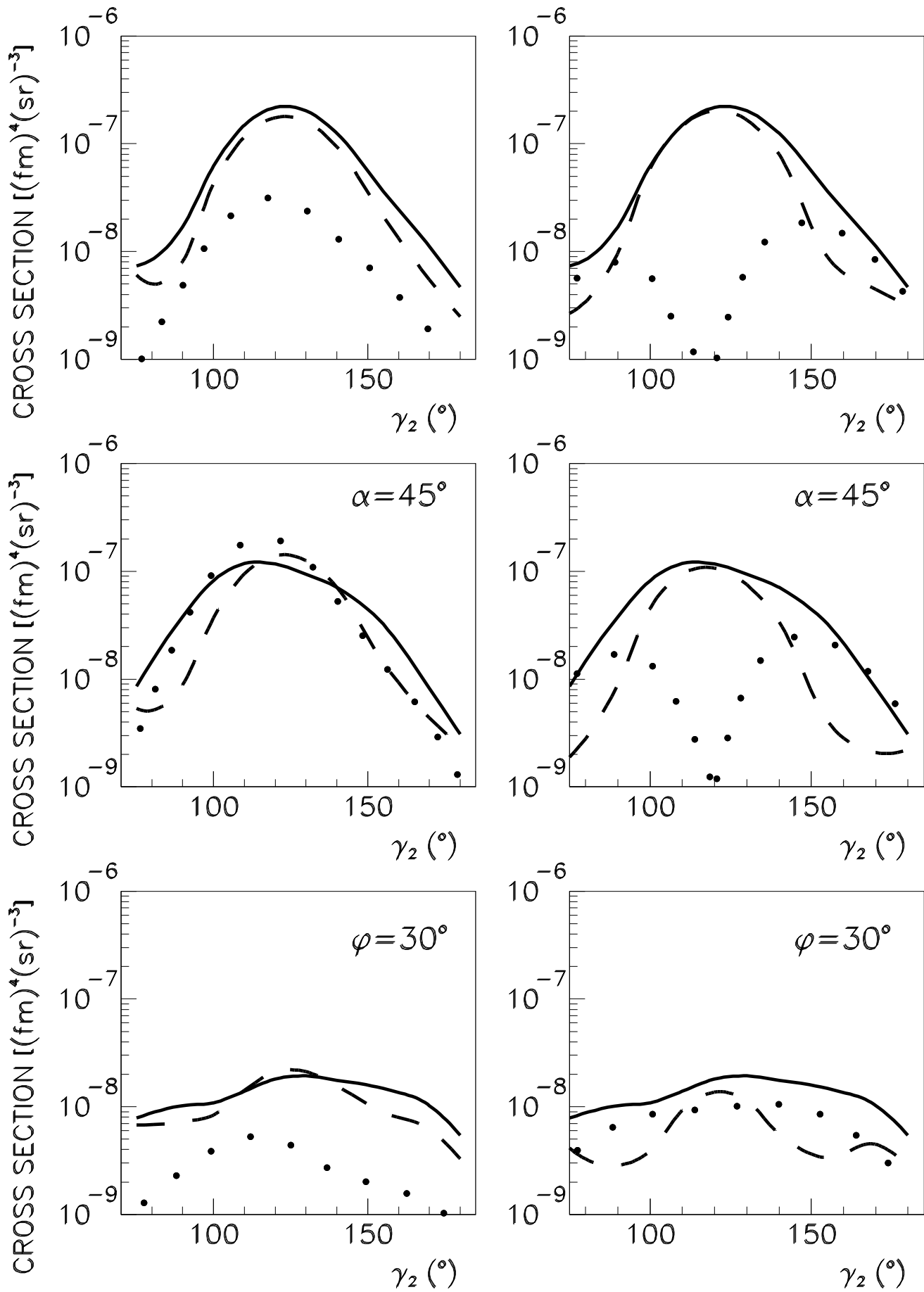


Fig. 4

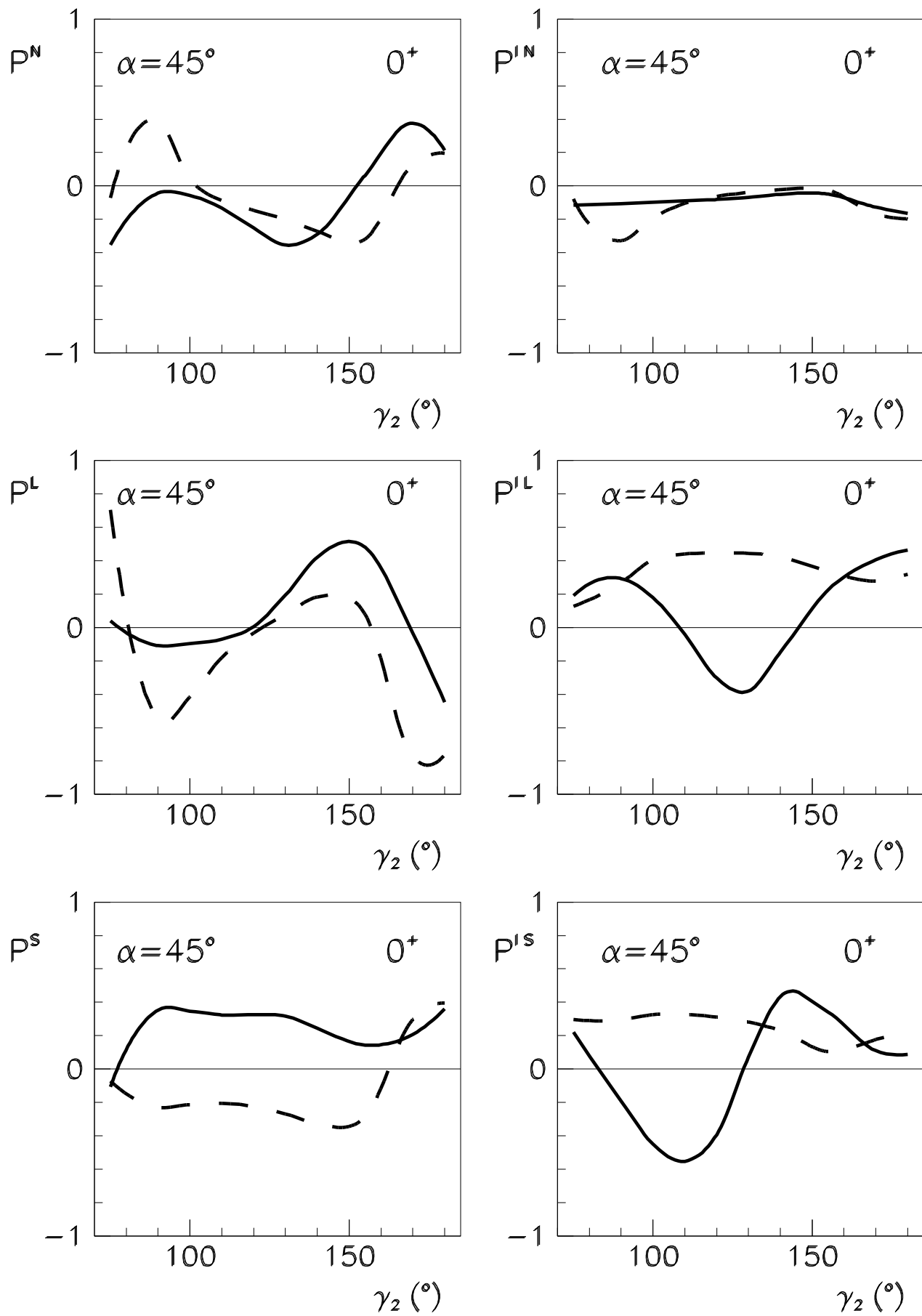


Fig. 5

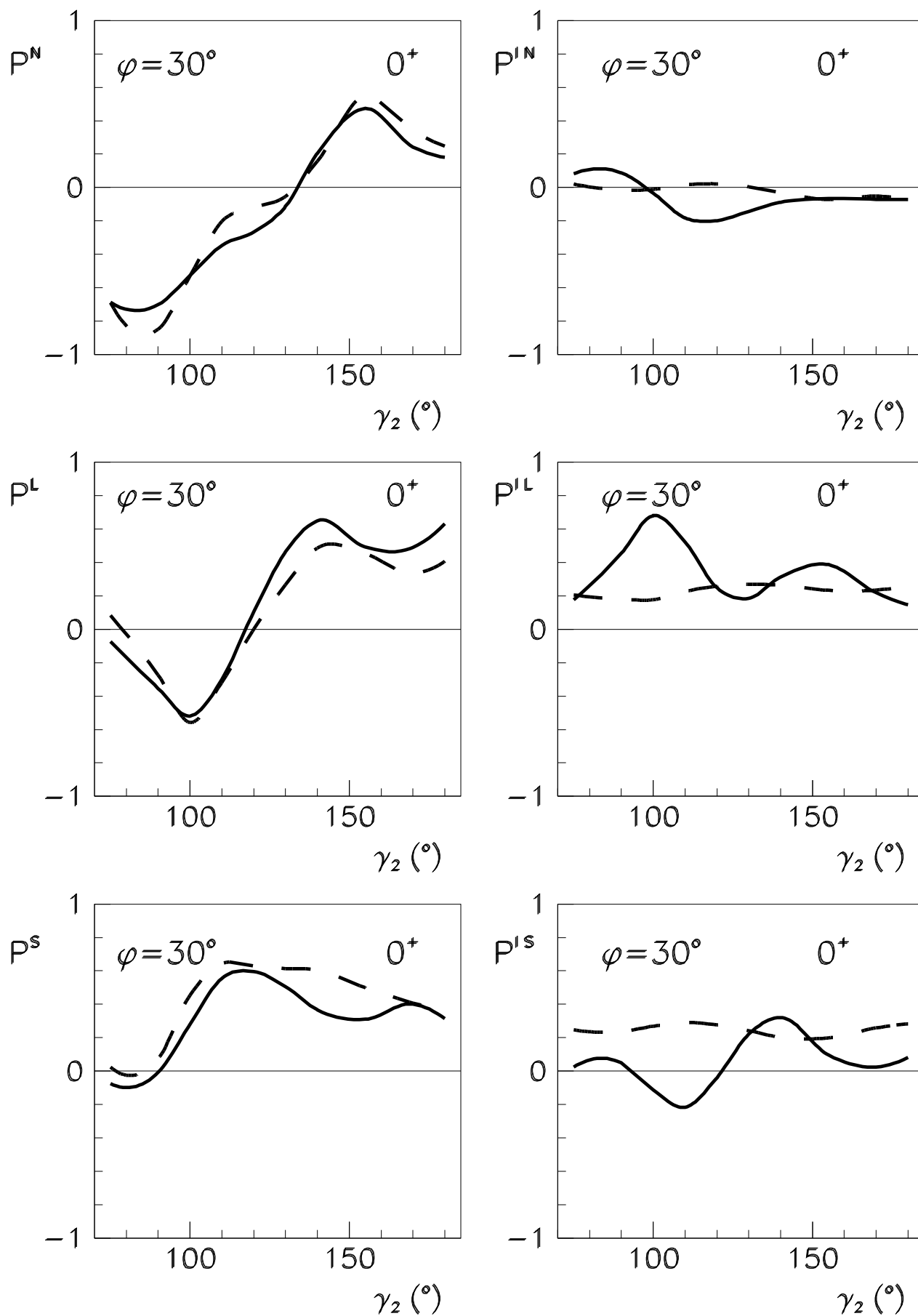


Fig. 6